OPEN ACCESS
IOP Publishing
Measurement Science and Technology
Meas. Sci. Technol. **34** (2023) 104003 (9pp)
https://doi.org/10.1088/1361-6501/ace542

Fiber-coupled phosphor thermometry for wall temperature measurements in a full-scale hydrogen gas turbine combustor

Patrick Nau[1,*], Andre Müller[2], Niklas Petry[1], Sebastian Nilsson[3], Torsten Endres[2], Mattias Richter[3] and Benjamin Witzel[4]

[1] German Aerospace Center (DLR), Institute of Combustion Technology, Pfaffenwaldring 38–40, 70569 Stuttgart, Germany
[2] Institute for Energy and Materials Processes—Reactive Fluids (EMPI), University of Duisburg-Essen, 47057 Duisburg, Germany
[3] Combustion Physics, Department of Physics, Faculty of Engineering, Lund University, Professorsgatan 1, 223 63 Lund, Sweden
[4] Siemens Energy, 45473 Mülheim ADR, Germany

E-mail: patrick.nau@dlr.de

Received 27 February 2023, revised 4 May 2023
Accepted for publication 7 July 2023
Published 17 July 2023

Abstract

Online wall temperatures were measured with fiber-coupled phosphor thermometry in a full-scale gas turbine combustor. The combustor was operated with natural gas and up to 100 vol% hydrogen at engine-relevant conditions. Two phosphors were tested for this application, namely YAG:Dy and YAG:Tm;Li. Although YAG:Tm;Li seemed to be the most promising phosphor for this application, it turned out to be incompatible with the used setup due to a strong interfering signal generated by the laser in the used fiber setup. A strategy to compensate for interferences from flame emissions during natural gas operation was developed. With this strategy it was possible to obtain single-shot temperature measurements at 15 Hz and a precision of 2–7 K for a 1 s average.

Keywords: phosphor thermometry, hydrogen combustion, wall temperature, gas turbine

(Some figures may appear in colour only in the online journal)

1. Introduction

Hydrogen combustion in gas turbines will play a critical role in the transition toward sustainable energy production [1]. Renewable electricity generation is needed to mitigate anthropogenic climate change [2]. Because the energy production from these sources is often fluctuating (i.e. wind and solar power), additional flexible and dispatchable power generation is needed. The use of hydrogen as a fuel in gas turbines presents a promising solution, as hydrogen combustion produces no carbon dioxide, but only water as the main product. This makes it an attractive alternative to fossil fuels that release harmful greenhouse gases into the atmosphere. In addition, hydrogen can be produced through various methods, including renewable sources such as solar and wind power. This allows

* Author to whom any correspondence should be addressed.

for the creation of a closed-loop system where the energy used to produce the hydrogen can be generated from sustainable sources. The hydrogen is then stored or transported and burned in gas turbines to release the energy when needed.

Especially during the transition time from fossil fuels to sustainable fuels, gas turbines will be operated with different fuels or fuel mixtures. Because the combustion properties of the different fuels can differ significantly, gas turbines with a fuel flexible burner design must be developed [3]. Knowledge of wall temperatures is important for the development of gas turbine combustors as it directly impacts the efficiency and performance of the turbine. High wall temperatures can result in material degradation and decreased engine lifetime, while low wall temperatures can lead to poor combustion and decreased engine performance. Accurate measurement and control of wall temperatures is therefore crucial in optimizing the performance of gas turbine combustors and ensuring their safe and efficient operation.

There are various online and offline techniques for measuring wall temperatures in gas turbine combustors. While offline techniques only provide the maximum temperature, online techniques deliver the actual temperature during the combustor test. Thermocouples are a widely used online technique. They can provide temperatures with good precision. However, it is intrusive and therefore not suited for certain applications. The lifetime of thermocouples installed in a combustion chamber is also very short. For the development of gas turbine combustors they are widely used, but usually only temperatures on the combustor outside walls are monitored. However, exact knowledge of the inside wall temperatures is crucial. These walls are usually coated with a thermal barrier coating (TBC) to protect the metal walls from excessive heat.

Phosphor thermometry has proven to provide temperatures with good precision and accuracy for this application [4–7]. This technique uses luminescent particles, which are excited with a light source, usually a laser. The emitted light is then analyzed to obtain the temperature utilizing the lifetime of the phosphorescence or the emission spectrum. Because optical access is often very limited in large test rigs with engine-relevant dimensions and boundary conditions, a fiber-coupled setup is often the only practical solution to perform optical measurements. Fiber-coupled phosphor thermometry in gas turbine combustors has already been demonstrated, for example, on stator vanes [8, 9] or the wall of a large-scale gas turbine combustor [10].

Our measurements recently performed at the Siemens Clean Energy Center (CEC) test facility were mainly limited by interference from flame emissions [10]. Therefore, temperatures could only be obtained with a rather long measurement time of 6.7 s for each data point. The aim of the current study was to improve the temporal resolution to at least 1 s. Therefore we implemented a background subtraction strategy to minimize the influence from flame emissions, which probably stemmed mainly from CO_2^*. To improve the signal level we tested two phosphors, namely YAG:Dy and YAG:Tm;Li. These phosphors have been used before in several studies for high-temperature applications [9, 11–13]. Both phosphors were compared in a recent investigation and their temperature and oxygen sensitivity, accuracy and signal intensity were analyzed [14].

2. Experimental

2.1. Test facility and optical probe

Wall temperature measurements were performed in a Siemens high-pressure combustion test rig operated at the Siemens CEC test facility in Ludwigsfelde near Berlin. Three testbeds are available at the facility with exchangeable combustion rigs. The combustion rigs allow tests of gas turbine combustors at engine-relevant thermodynamic boundary conditions, i.e. maximum rig pressures of 40 bar and a maximum air inlet temperature of 870 K at air mass flows up to 50 kg s^{-1}.

The combustion test rig consists of a pressure vessel containing an exchangeable flow box to mimic the conditions in the gas turbine. Flowbox and burners can be exchanged to test different configurations. A back pressure valve is used to adjust the rig pressure to account for different engine pressure levels.

To gain optical access to the combustor an optical probe was used. The design was similar to the one used before [10], but was adapted to the test rig used in this investigation. No modifications to the flowbox or other machine components were required. As a result, the probe design has become more compact and rigid. A schematic of the setup is shown in figure 1 and a photograph of the probe is presented in figure 2.

Like in [10], it was found that the concept of the tube-in-tube heat exchanger could also be optimally used for this probe. The inner tube served as the inflow, supplying cooling water to the sensitive fiber and optics and discharging it in a circuit through the outer tube. Inlet and outlet water temperatures were monitored with thermocouples. The fiber was further enclosed in a Teflon hose inside the probe for additional protection.

The probe consists of a long rigid tube, a modular probe head connected to the tube with a short flexible tube, a big stuffing box and the rear part with all external connections. The bare fiber is sealed with a small stuffing box against the cooling water inside the probe. The fiber in the probe was then coupled with a long fiber between probe and measurement container via an SMA mating sleeve (ADASMA, Thorlabs). This simplified installation of the probe and changing the fiber, e.g. if the fiber breaks and has to be replaced, compared to a setup with only one continuous fiber between probe and container.

A short flexible tube was welded onto the rigid tube to allow for precise insertion of the probe into the combustor adapter and to compensate for any thermal expansion. The additively manufactured modular probe head made of Inconel 625 was screwed onto the flexible tube and sealed with pressure-filled metal O-rings. An adapter built by additive manufacturing was welded on the outside of the complex geometry of the combustor outside wall to hold the probe head. The adapter features internal channels for nitrogen that are used to cool the

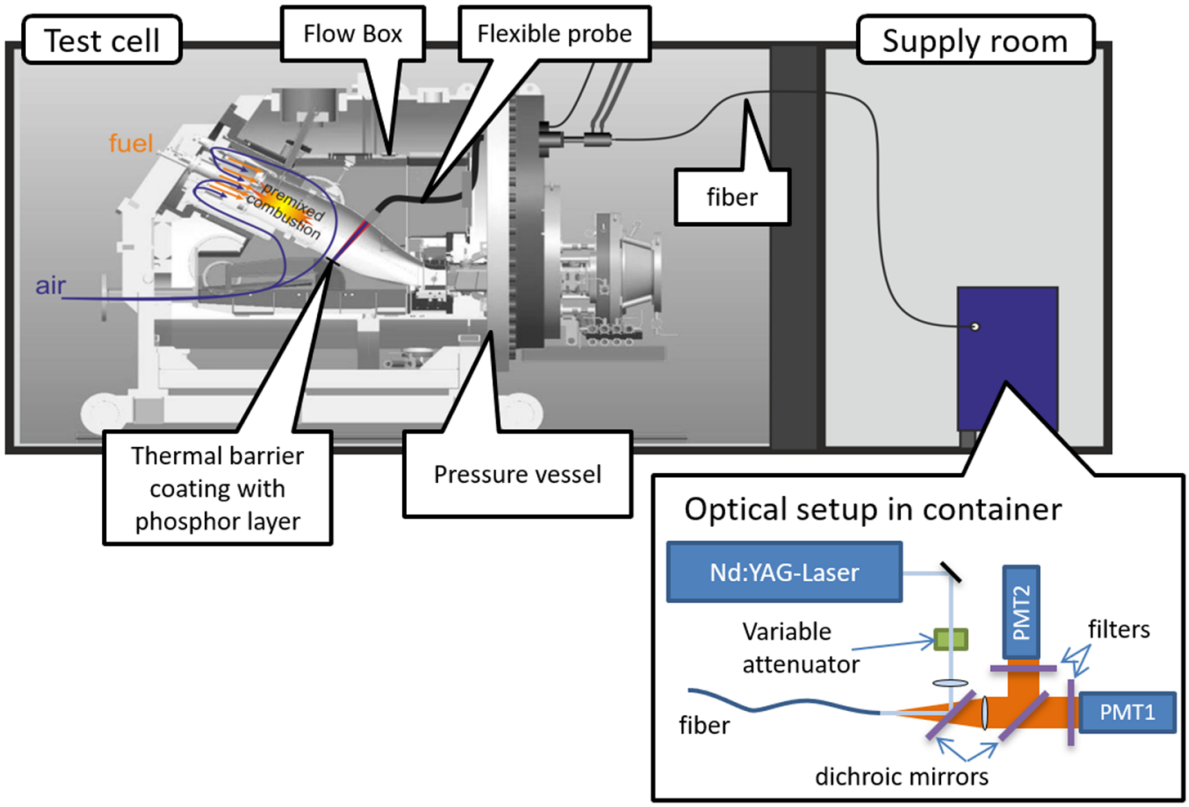

Figure 1. Schematic of the high-pressure test rig, optical probe and optical setup in the measurement container.

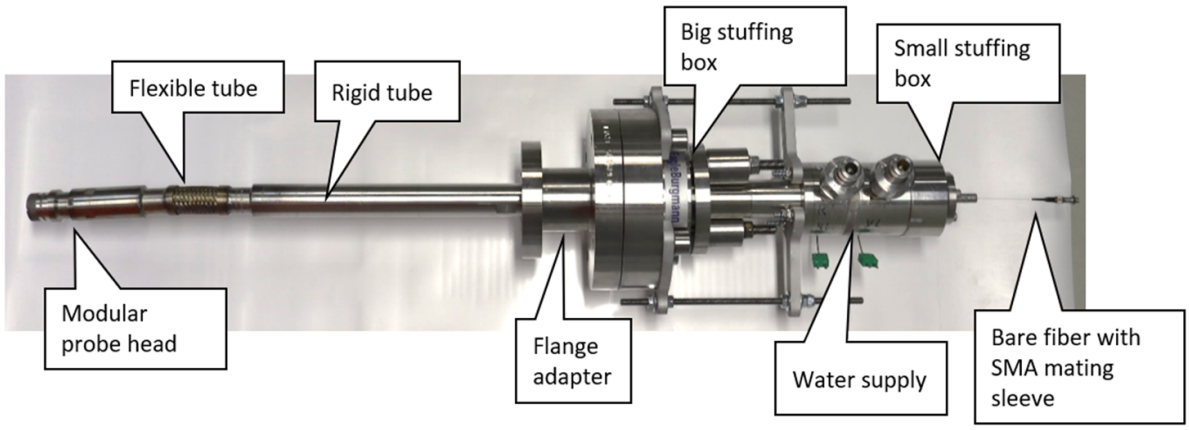

Figure 2. Photograph of the assembled optical probe with its components.

modular probe head and to purge the sapphire window to prevent contamination and deposits. An optical holder made of Ampcoloy is screwed into the probe head. This holder contains the glued-in lens for laser excitation and signal collection.

2.2. Measurement setup

A mobile measurement container was used for the wall temperature measurements. The container simplifies setting up the system at the test rig and was already used for a previous measurement campaign [10]. The Laser beam from a Nd:YAG-Laser (Innolas GmbH, Spitlight600, 15 Hz repetition rate, 6 ns pulse length at 355 nm) was coupled into a large core optical fiber (FVA, 1000 µm core diameter, Laser Components GmbH) with a lens ($f = +75$ mm). The laser light was recollimated in the optical probe with a lens ($f = +20$ mm). Due to the viewing angle of the probe an oval laser spot with about 12×16 mm was illuminated on the opposing site of the combustor wall. The used laser energy in front of the optical fiber was about 1.1 mJ resulting in a laser energy density of about 0.6 mJ cm^{-2} on the phosphor coating.

The phosphorescence emitted from the surface was captured with the same optics in the probe and travels back through the same optical fiber. In the measurement container

the phosphorescence light passed a dichroic mirror (Thorlabs, HBSY234), to separate it from the laser light. The light was then collimated with a lens. A second dichroic mirror (Thorlabs, DMLP425R, longpass filter) was used to guide light at wavelengths below 425 nm to a photomultiplier tube (PMT) equipped with a bandpass filter at 410 nm (Thorlabs, FBH410-10 center wavelength 410 nm, bandwidth 10 nm). The light transmitted through the dichroic mirror (wavelengths above 425 nm) passed a bandpass filter at 458 nm (Edmund Optics, 65142, center wavelength 458 nm, bandwidth 10 nm) and was detected with a further PMT. Both PMTs (Hamamatsu, H11526-20-NF) were gated to exclude the beginning of the Signal (0.2 µs for YAG:Tm;Li and 5 µs for YAG:Dy), which is strongly affected by broadband emission caused by the laser fiber coupling. This effect has been reported before for similar single fiber setups [8, 9]. The PMT behind the 410 nm filter was intended to capture broadband background emissions, e.g. from CO_2^*, while the second PMT behind the 458 nm filter will capture the phosphorescence signal.

The coating and calibration procedure was similar to the one reported before [10]. Thin phosphor coatings were spray painted on the surface using an air brush (Badger 100). We aimed for a thickness of about 20 µm, which has shown to cause minimal errors due to thermal gradients [15, 16]. Because direct determination of the thickness was not possible on the combustor wall, small steel samples were coated with the same procedure and the thickness was measured with a coating thickness gauge (Sauter, TE 1250-0.1FN). Several layers were sprayed to increase homogeneity and dried with a heat gun. A mixing ratio of 1 g phosphor powder (YAG:Tm(1%);Li(0.1%) and YAG:Dy(2%), Phosphor Technology) in 10 ml binder (Zyp coatings) was used. LRC binder was used for YAG:Dy and YAG binder for YAG:Tm;Li. On the TBC coated combustor wall an area of about 50 mm in diameter was coated. For calibration measurements a small disc of TBC material with a thickness of about 1 mm was coated in the same way as in the combustor. Calibration measurements were performed in an optically accessible furnace (LAC, VP 10/16, Boldt Wärmetechnik GmbH) with a thermocouple (type B) placed on the back of the TBC sample.

3. Results and discussion

3.1. Phosphor selection and calibration

YAG:Dy and YAG:Tm;Li were recently investigated as the most promising phosphors for high-temperature measurements in gas turbines [14]. YAG:Tm;Li shows higher temperature sensitivity and about one order of magnitude higher signal intensity than YAG:Dy. In addition, their oxygen sensitivity was lower. This is important because the oxygen concentration in a gas turbine is often not exactly known. However, for YAG:Dy, this is mainly a concern for oxygen levels below 5%. The typical oxygen concentrations in the investigated flames were above 6%. For these oxygen levels, the effect was well below the measurement precision and can be neglected in this investigation.

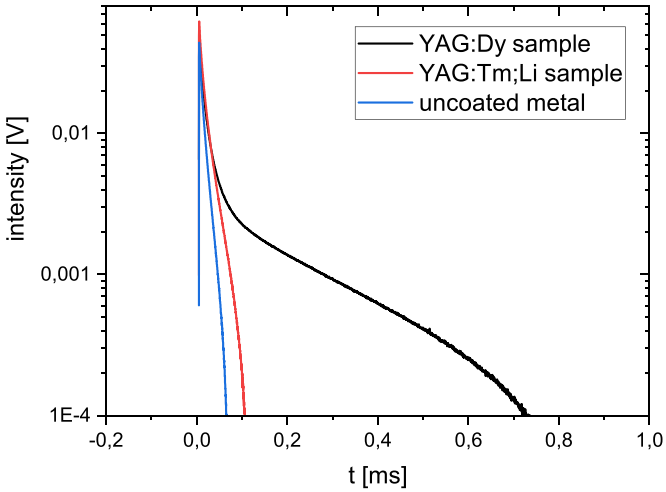

Figure 3. PMT signals averaged over 600 laser shots at room temperature of the two investigated phosphors coated on a TBC substrate and an uncoated metal wall measured using the fiber optical probe at the test rig.

Calibration measurements for both phosphors are shown in figure 4(c). For the investigated temperatures between 1300 and 1650 K the decay rates of YAG:Tm;Li range from about 10 µs down to 200 ns. The shorter decay rates are somewhat difficult to measure with the used single fiber setup because, as mentioned before, the beginning of the decay curve is covered with an intense spike caused by the laser inside the fiber. This spike is orders of magnitude stronger than the phosphorescence and is spectrally quite broadband, with the strongest emission at approximately 470 nm. This was probably due to the fluorescence of the quartz material inside the fiber. Due to the spectral structure, it was not Raman scattering, as reported for a similar setup before [9], while quartz can show a similar fluorescence spectrum [17].

Owing to the broadband nature of the interfering fluorescence signal, it is not possible to filter it spectrally. Therefore, the easiest solution is to use gating to exclude the beginning of the decay curve. For our setup a gate of at least 200 ns was necessary to filter out the fluorescence. Furthermore, the risetime of the used PMT (70 ns) has to be considered as well. Therefore a significant amount of phosphorescence signal is filtered out by the gate at high temperatures. However, for the investigated temperatures it was possible to perform measurements in an oven and the peak signal strength was still stronger than for YAG:Dy. Therefore YAG:Tm;Li was our preferred candidate for wall temperature measurements in the combustor.

After the installation of the optical probe in the combustor, a strong interfering signal was present with almost the same decay rate as that of YAG:Tm;Li. This signal was different from the much shorter fluorescence signal reported above. To find the origin of this signal, tests were performed on TBC samples coated with YAG:Tm;Li, YAG:Dy, and uncoated metal (figure 3). While on the uncoated metal

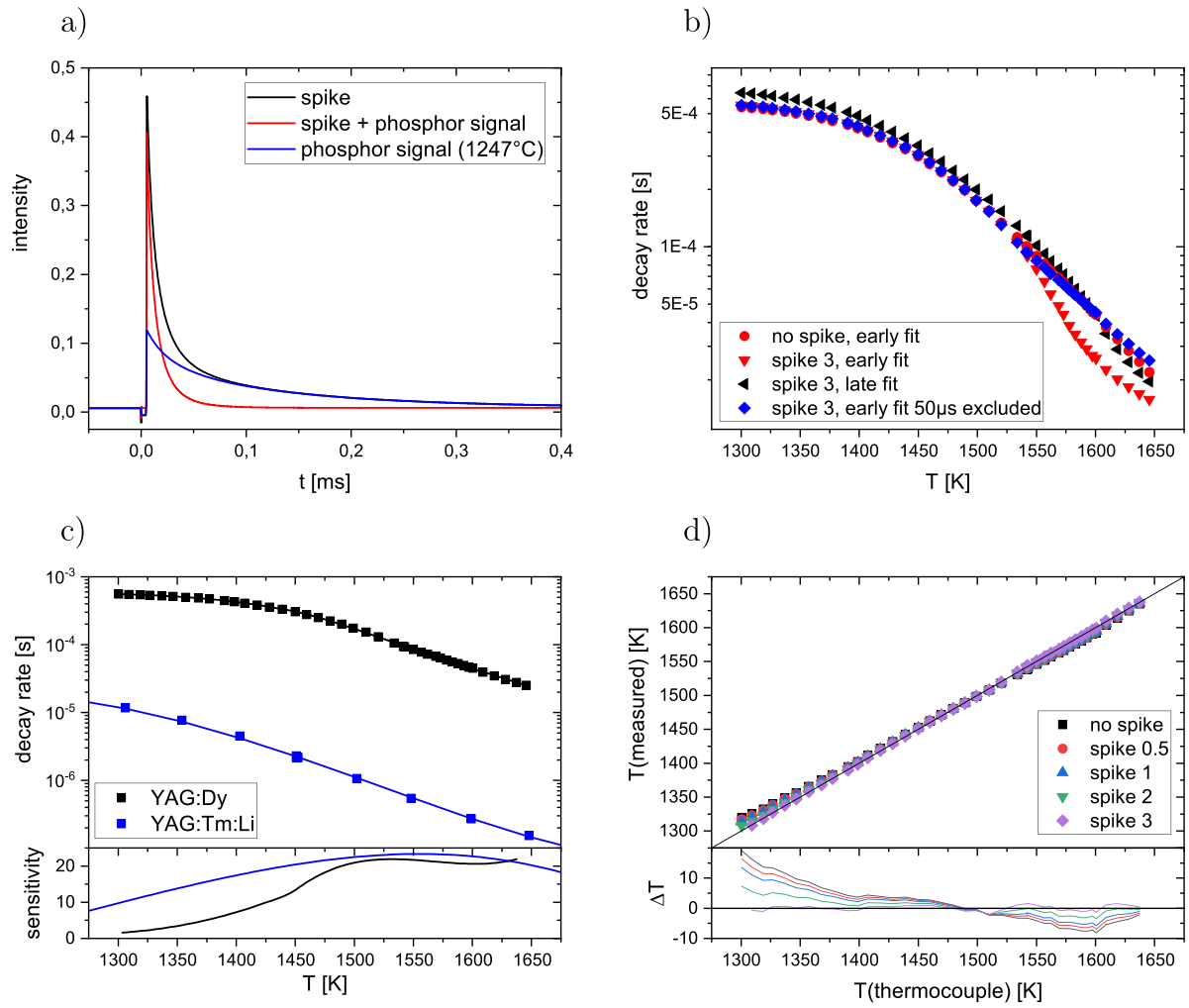

Figure 4. Calibration and influence of the spike on data evaluation. (a) Exemplary decay curve of YAG:Dy with and without spike. (b) Obtained decay rates for YAG:Dy for different fitting windows with and without spike. (c) Calibration data and temperature sensitivity for YAG:Dy and YAG:Tm:Li. (d) Temperature error for different ratios of spike to phosphor signal amplitude for YAG:Dy.

no phosphorescence signal should be present, the interfering signal was still present. Further tests showed that the signal was only present when the fiber cables were joined together with mating sleeves. However, initial tests in the lab were performed with fiber cables with an air-gap-ferrule SMA connector. Using the air-gap-ferrule connector the signal was not present, therefore probably epoxy or some other material in the SMA connector of the used fiber caused the observed interfering signal. Unfortunately, no fiber with a different connector was available during the measurement campaign. Since the decay rate of this signal was about 13 µs, which is similar to YAG:Tm;Li at about 1300 K, and because the signal was more intense than the phosphorescence of the coating, measurements were impossible with YAG:Tm;Li. It should also be noted that the observed interfering signal is different from the fiber fluorescence mentioned before. The fluorescence is on a timescale of a few nanoseconds, while the interfering signal seems to be phosphorescence. The only solution for this measurement campaign was to use the phosphor YAG:Dy instead, whose phosphorescence decay time is almost two orders of magnitude longer (figure 4(c)). As can be seen in figure 3 the phosphorescence of YAG:Dy can be distinguished very well from the short interfering signal.

To investigate the influence of the spike on the data evaluation procedure for YAG:Dy, calibration measurements were performed in an oven. The same optical setup in the measurement container, but a different fiber (FG910UEC with air-gap-ferrule, Thorlabs) was used for these measurements. The interfering signal was not present in these measurements. Synthetic data sets were created with different amplitudes of the interfering spike (ratios of spike to phosphorescence amplitude α between 0.5 and 3). The signal measured on the uncoated metal (figure 3) was scaled and then added to the measured decay curves of the phosphor as can be seen exemplary in figure 4(a) for an amplitude ratio α of 3.

Different fitting routines were tested to evaluate any systematic errors caused by the spike. The adaptive fitting window approach was used to fit the decay curves [18]. In this approach the fitting window is defined by the decay time τ, with $c1 \times \tau$ defining the starting time of the fitting window

and $c2 \times \tau$ the end of the window. After iterative fitting τ converges. This approach has proven to be very useful when dealing with multi-exponential decay curves. Smaller values of $c1$ and $c2$ shift the window to the beginning of the pulse and therefore result in shorter values of τ. It is expected that an early fitting value is more strongly influenced by the interfering spike. However, if the fitting window is too late, the signal to noise ratio becomes too low to allow meaningful measurements, especially when single-shot measurements are desired.

In figure 4(b) results from three fitting routines for data without spike and with an spike amplitude ratio of three (similar to the amplitude at the test rig) are shown. The late fitting window is defined by $c1 = 1$ and $c2 = 4$, while the early fitting window is $c1 = 0.5$ and $c2 = 3$. In addition, the early fitting window was used and the first 50 µs were excluded from the fit. As can be seen, the late fit results in slightly longer decay rates as expected. Up to a temperature of about 1550 K the results from all fitting routines are very similar. At higher temperatures, and therefore shorter decay rates of the phosphor, the influence from the interfering spike becomes significant, especially for the early fitting window. The late fitting window and the approach with 50 µs excluded from the beginning of the curve are less affected. The results for these approaches are very similar to the data set without interfering spike. Because the late fitting window would have made single-shot measurements difficult due to the noise level present in single-shot decay curves, we used the approach with $c1 = 0.5$ and $c2 = 3$ and excluding the first 50 µs.

The calibration data sets for YAG:Dy and YAG:Tm;Li are shown in figure 4(c). For YAG:Dy the approach described above with the early fitting window and the first 50 µs excluded was used, while for YAG:Tm;Li the early fitting window was used. For YAG:Tm;Li only data without the interfering spike can be evaluated. As can be seen the sensitivity defined as $(d\tau/dT)/(\tau/T)$ of this phosphor is higher, especially for temperatures below 1475 K. A polynomial was fitted to the data to obtain a calibration curve.

Finally, the sensitivity of the approach for different spike amplitudes was tested. Using the calibration polynomial for YAG:Dy shown in figure 4(c), temperatures were calculated for the synthetic datasets with different spike amplitudes (figure 4(d)). The difference between the measured and actual temperatures ΔT increased as the spike amplitude α differed between the calibration and test datasets. At 1550 K (the highest temperature measured in the combustor) the sensitivity of the temperature error ΔT on the spike amplitude α was $d\Delta T/d\alpha = 2$ K. As the amplitude of the spike was also quite constant during the combustor measurements we assume a maximum error of 2 K (0.1%).

Several additional factors contribute to the total temperature measurement uncertainty. These can be divided into contributions from the calibration procedure and the decay time measurement in the experiment itself. Similar to Peral *et al* we identified the thermocouple measurement during the calibration and the decay time measurement as the main contribution to measurement uncertainty [19]. Systematic errors from differences in the experimental setup between experiment and calibration were greatly reduced by using the same optics where possible and the same electronics. The uncertainty from the reference thermocouple measurement in the calibration oven was estimated to 0.5%. The polynomial fitted to the calibration data (compare figure 4(c)) causes an error due to interpolation between data points of about 0.5 K.

The precision resulting from the decay time measurement was estimated from the standard deviation individual measurements (300 laser shots) at a constant temperature in the oven. Using the early fitting window with the first 50 µs excluded, the precision was between 7 K (0.5%) at 1500 K and 27 K (2%) at 1325 K for single shot measurements. Using a measurement time of 1 s (averaging of 15 laser shots) the error reduced to 2 K (0.1%) and 7 K (0.5%) respectively. The late fitting window resulted in a 50% higher error (3–11 K at 1 s measurement time).

3.2. Data evaluation

A second PMT was installed to capture the background emission. The strong fluctuations in the background level distort the phosphorescence signal and prevented single-shot measurements in our previous investigation [10]. The wavelength of the bandpass filter for the second PMT was selected to 410 nm. This wavelength is still relatively close to the detected emission line (458 nm) and both phosphors show no significant emission at 410 nm, while CO_2^* emission is still very prominent at this wavelength [20].

Exemplary signals from both PMTs during combustor operation with natural gas are shown in figure 5. The black line (PMT1) shows signal from fluctuating background, the phosphor emission and the spike at the beginning of the decay curve described before. The blue line (PMT2) also shows the spike and the fluctuating background, but no phosphorescence signal. The signal of PMT2 was therefore smoothed by a Savitzky–Golay filter and scaled to the signal of PMT1. The section covering the spike was excluded for this procedure, because this region was not used for the decay time fitting and the relative intensities of background signals and spike are unknown for both PMTs. A subtraction of the spike was therefore not possible. After subtraction of the smoothed background signal the corrected curve (red) was used for further data evaluation. As can be seen the corrected curve only shows the phosphorescence decay curve and is not distorted by the fluctuating background any more. The complete process was automated with a LabVIEW program to allow data evaluation of single-shot laser pulses.

Temperatures obtained from single-shot curves with and without background subtraction are shown in figure 5(b). As can be seen the distortion of the decay curve due to the fluctuating background results in a large error in the obtained temperatures. After background subtraction the error is greatly reduced with a standard deviation of less than 10 K. It is also interesting to see that during hydrogen operation the fluctuating background is not present which further supports the hypothesis, that the background is mainly CO_2^*, which is obviously not present in a hydrogen flame. The background subtraction procedure does also not cause a systematic shift of the obtained temperature. This can be seen by comparing the blue and black

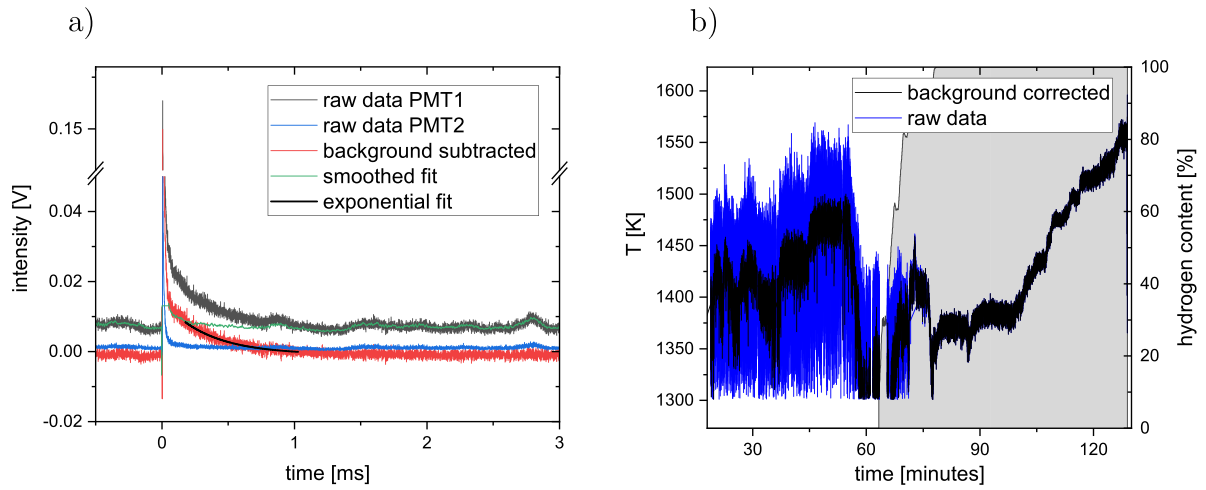

Figure 5. (a) Procedure for background subtraction. Exemplary signals from both PMTs (black and blue), smoothed and scaled signal from PMT2 (green), PMT1 signal with background subtracted (red). (b) Temperatures obtained for each laser pulse with (black) and without (blue) background subtraction procedure. Hydrogen content is shown in gray.

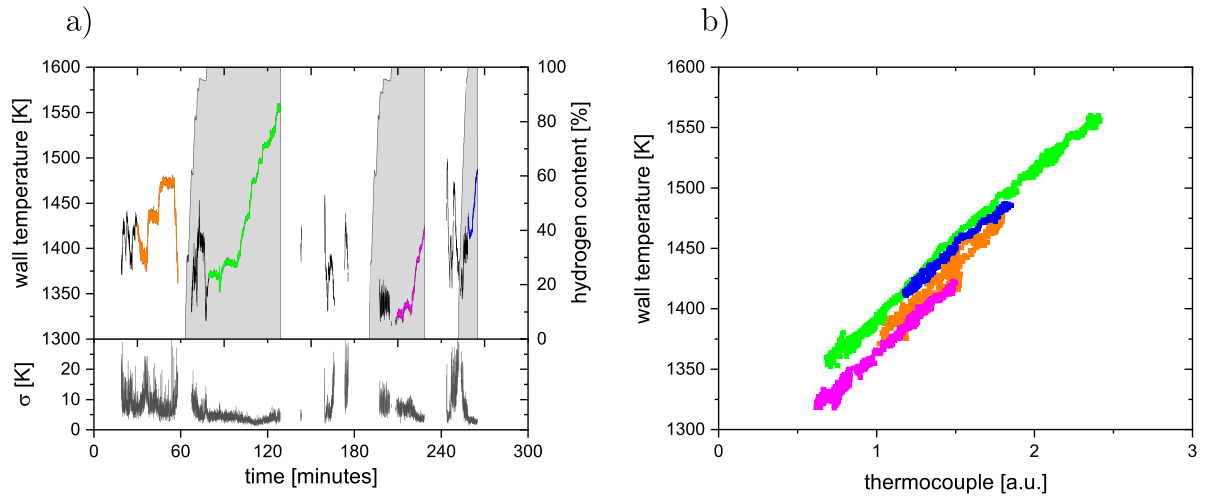

Figure 6. (a) Measured wall temperatures averaged over 1 s (upper plot) and corresponding standard deviation σ (lower plot) plotted against the measurement time. Hydrogen content is shown as dotted area. (b) Wall temperatures of four selected time windows plotted against a thermocouple. The color coding corresponds to the left plot.

lines. These lines match perfectly for the hydrogen conditions, while during natural gas operation only averaged values could be compared which also match.

3.3. Wall temperature measurements

Wall temperatures obtained on the combustor wall are shown in figure 6(a). The temperatures have been averaged over 1 s and the corresponding standard deviation is shown in the lower part of the plot. The burner was ignited with natural gas and then the hydrogen content (indicated by the dotted region) was increased up to 100 vol%. The conditions were then gradually changed until flashback was detected and the burner was shut off. This was repeated three times for the measurement day. Shutdown of the burner comes with an immediate cooling of the combustor wall, clearly visible in figure 6(a) at 12:40, 14:20 and 14:55. The temperature is very quickly (within about three laser shots, or 0.2 s) below the lower temperature limit of the used phosphor of about 1300 K (compare figure 4(c)). The maximum temperature measured was 1555 K, which is well in the region where YAG:Dy shows highest temperature sensitivity. During operation with natural gas the standard deviation is about a factor of two higher than during hydrogen operation due to the interfering flame emissions mentioned above, while during hydrogen operation the standard deviation is similar to the oven measurements (section 3.1) resulting in a precision of 2–7 K for 1 s averaging.

The measured inside wall temperatures were compared with a thermocouple located on the outside of the combustor wall close to the measurement position (figure 6(b)). Especially the temperatures on the outside surface are affected by variations in the air flow rate and temperature. Therefore, for this comparison only those time windows were used were

the burner was operated stable and i.e. conditions after ignition and during power up were excluded. These time windows are marked in orange, green, magenta and blue in both figures. Due to confidentiality only normalized thermocouple values are shown here. These values will allow to compare relative trends. A detailed analysis of heat conduction was beyond the scope of this investigation. It is clearly visible that a direct linear relationship exists between the inside wall temperature from phosphor thermometry and the outside temperature measured with the thermocouple. Slight differences can be seen for the four time windows. While the slope is very similar for all four cases an offset of up to 30 K can be observed. This can be explained by differences in the measurement conditions resulting in different temperature gradients between TBC surface and combustor outside metal wall measurement location. Inside and outside measurement locations were not exactly on opposite sides of the combustor wall (distance about 5 cm). Therefore both values will react slightly different on variations in flame position and cooling air flow.

4. Conclusion

Online wall temperatures were successfully measured with fiber-coupled phosphor thermometry in a full-scale high-pressure gas turbine combustor. The burner was operated with natural gas and up to 100 vol% hydrogen. Compared to a previous investigation [10] the signal quality was improved significantly and single-shot measurements at 15 Hz were possible. This was mainly achieved by using a second PMT to capture interfering background from flame emissions at a wavelength where no emission lines from the used phosphor were present. During hydrogen operation of the burner almost no interference from flame emissions was present. This supports the assumption, that the interference is mainly attributed to CO_2^*.

Inside wall temperatures were compared with values from a thermocouple located at the outside of the combustor metal wall. A linear relationship was observed with a similar slope for all investigated measurement conditions. An offset between different conditions of up to 30 K can be attributed to differences in flow conditions.

Measurements were successful using YAG:Dy, while the phosphor YAG:Tm;Li failed for the used setup. The reason was an interfering signal on a timescale similar to YAG:Tm;Li phosphorescence generated by the fiber–fiber-coupling using an SMA mating-sleeve. This could be avoided in further measurements by using a different fiber and would make it possible to use YAG:Tm;Li, which should give an even better signal intensity and higher temperature sensitivity. This provides the potential to further enhance the precision of 2–7 K achieved here for a 1 s averaging time.

Data availability statement

All data that support the findings of this study are included within the article (and any supplementary files).

Acknowledgments

This project has received funding from the European Union's Horizon 2020 research and innovation programme under Grant Agreement Nos. 884229 and 852394. The authors gratefully acknowledge Siemens Energy AG for their support and permission to publish this paper.

ORCID iDs

Patrick Nau https://orcid.org/0000-0002-4403-8065
Niklas Petry https://orcid.org/0000-0001-9030-104X
Sebastian Nilsson https://orcid.org/0000-0002-6953-8736
Torsten Endres https://orcid.org/0000-0001-8100-3921
Mattias Richter https://orcid.org/0000-0002-9914-7218

References

[1] Öberg S, Odenberger M and Johnsson F 2022 Exploring the competitiveness of hydrogen-fueled gas turbines in future energy systems *Int. J. Hydrog. Energy* **47** 624–44
[2] Intergovernmental Panel on Climate Change 2014 *Climate Change 2014: Synthesis Report. Contribution of Working Groups I, II and III to the Fifth Assessment Report of the Intergovernmental Panel on Climate Change* ed Core Writing Team, R K Pachauri and L A Meyer (IPCC) (available at: www.ipcc.ch/report/ar5/syr/)
[3] Huth M and Heilos A 2013 Fuel flexibility in gas turbine systems: impact on burner design and performance *Modern Gas Turbine Systems* ed P Jansohn (Woodhead Publishing) ch 14, pp 635–84
[4] Allison S W and Gillies G T 1997 Remote thermometry with thermographic phosphors: instrumentation and applications *Rev. Sci. Instrum.* **68** 2615–50
[5] Aldén M, Omrane A, Richter M and Särner G 2011 Thermographic phosphors for thermometry: a survey of combustion applications *Prog. Energy Combust. Sci.* **37** 422–61
[6] Brübach J, Pflitsch C, Dreizler A and Atakan B 2013 On surface temperature measurements with thermographic phosphors: a review *Prog. Energy Combust. Sci.* **39** 37–60
[7] Allison S W 2019 A brief history of phosphor thermometry *Meas. Sci. Technol.* **30** 072001
[8] Noel B W, Borella H M, Lewis W, Turley W D, Beshears D L, Capps G J, Cates M R, Muhs J D and Tobin K W 1991 Evaluating thermographic phosphors in an operating turbine engine *J. Eng. Gas Turbines Power* **113** 242–5
[9] Eldridge J I, Allison S W, Jenkins T P, Gollub S L, Hall C A and Greg Walker D 2016 Surface temperature measurements from a stator vane doublet in a turbine afterburner flame using a YAG:Tm thermographic phosphor *Meas. Sci. Technol.* **27** 125205
[10] Nau P, Görs S, Arndt C, Witzel B and Endres T 2020 Wall temperature measurements in a full-scale gas turbine combustor test rig with fiber coupled phosphor thermometry *J. Turbomach.* **143** 011007
[11] Regmi A R, Allison S W, Olenick K and Sabri F 2021 High temperature phosphor thermometry with YAG:Dy and LED excitation on flexible YSZ ceramic ribbons *MRS Commun.* **11** 322–9
[12] Nau P, Yin Z, Geigle K P and Meier W 2017 Wall temperature measurements at elevated pressures and high temperatures in sooting flames in a gas turbine model combustor *Appl. Phys.* B **123** 279

[13] Jovicic G, Zigan L, Will S and Leipertz A 2015 Phosphor thermometry in turbulent hot gas flows applying Dy:YAG and Dy:Er:YAG particles *Meas. Sci. Technol.* **26** 015204
[14] Nilsson S, Feuk H and Richter M 2023 High temperature thermographic phosphors YAG:Tm;Li and YAG:Dy in reduced oxygen environments *J. Lumin.* **256** 119645
[15] Knappe C, Algotsson M, Andersson P, Richter M, Tunér M, Johansson B and Aldén M 2013 Thickness dependent variations in surface phosphor thermometry during transient combustion in an HCCI engine *Combust. Flame* **160** 1466–75
[16] Pilgrim C C, Feist J P and Heyes A L 2013 On the effect of temperature gradients and coating translucence on the accuracy of phosphor thermometry *Meas. Sci. Technol.* **24** 105201
[17] Neal N J, Jordan J and Rothamer D 2013 Simultaneous measurements of in-cylinder temperature and velocity distribution in a small-bore diesel engine using thermographic phosphors *SAE Int. J. Engines* **6** 300–18
[18] Brübach J, Janicka J and Dreizler A 2009 An algorithm for the characterisation of multi-exponential decay curves *Opt. Lasers Eng.* **47** 75–79
[19] Peral D, Castillo D, Araguas-Rodriguez S, Yañez-Gonzalez A, Pilgrim C, Karagiannopoulos S, Feist J P and Skinner S 2019 Reliable temperature measurement with thermal history paints: an uncertainty estimation model *Proc. ASME Turbo Expo 2019, Volume 6: Ceramics; Controls, Diagnostics, and Instrumentation; Education; Manufacturing Materials and Metallurgy* (https://doi.org/10.1115/GT2019-92087)
[20] Goers S, Witzel B, Heinze J, Stockhausen G, van Kampen J, Schulz C, Willert C and Fleing C 2014 Endoscopic chemiluminescence measurements as a robust experimental tool in high-pressure gas turbine combustion tests *Proc. ASME Turbo Expo 2014, Volume 4B: Combustion, Fuels and Emissions* (https://doi.org/10.1115/GT2014-26977)